This is an open access article published under a Creative Commons Attribution (CC-BY) License, which permits unrestricted use, distribution and reproduction in any medium, provided the author and source are cited.

ACS AUTHORCHOICE

ACS OMEGA

Article

Cite This: ACS Omega 2020, 5, 1782−1788

Study on the Colorimetry Properties of Transparent Wood Prepared from Six Wood Species

Yan Wu,*[,†] Jichun Zhou,[†] Qiongtao Huang,[‡] Feng Yang,*[,§] Yajing Wang,[†] Xinmu Liang,[†] and Jinzhu Li[†]

[†]College of Furnishings and Industrial Design, Nanjing Forestry University, Nanjing 210037, China

[‡]Department of Research and Development Center, Yihua Lifestyle Technology Co., Ltd., Shantou 515834, China

[§]Fashion Accessory Art and Engineering College, Beijing Institute of Fashion Technology, Beijing 100029, China

ABSTRACT: Transparent wood (TW) was prepared by directly impregnating the wood cell wall and cavity with index-matched prepolymerized methyl methacrylate (MMA). In this process, lignin is retained compared with the preparation of transparent wood in the past, making the production faster and more energy-efficient. The innovation lies in that the prepared transparent wood retains the natural color and texture of the wood while transmitting light, especially under the illumination of a specific light source, which exist as the special visual effects. In order to enhance the practicality of the research and effectively expand the types of home decoration materials, six common wood species with different densities were selected in the experiment. Then the characteristics and mechanisms of wood, that is, color difference, light transmittance, microstructure, changes of chemical functional groups, and tensile strength, before and after PMMA impregnating were compared and analyzed. It is concluded that the light transmittance and mechanical properties of the wood have been improved, and a good synergistic effect between wood and PMMA has been confirmed by the analysis of scanning electron microscopy and infrared spectroscopy. The above highlights make pervious to transparent wood, which has the potential as an excellent functional decorative material.

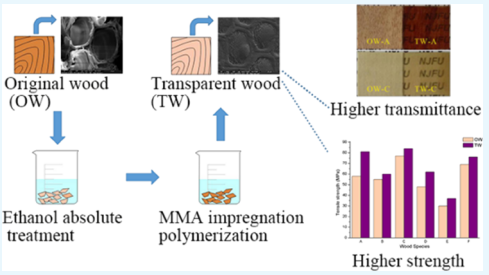

1. INTRODUCTION

Wood is a widely used structural material with excellent mechanical properties due to its unique natural growth structure.[1] At the same time, wood is also a good home decoration material owing to its natural texture and color. Because of its many advantages, powerful functions, and wide applications, wood attracts people to explore and study its mechanism, including its modification, in order to broaden more functions and uses. Among them, transparent wood as an emerging result of wood modification is entering the people's field of vision with the advantages of light weight, environmental protection, and light transmission.

Li et al.[2] removed the strongly light-absorbing lignin component from the balsa wood and obtained a nanoporous wood template. Optically transparent wood with transmittance as high as 85% and haze of 71% was obtained by bulk infiltration of refractive-index-matched, prepolymerized methyl methacrylate (MMA) in the above wood template. Based on good synergic action between the delignified wood template and PMMA, transparent wood has high transparency, strength, and modulus; meanwhile, transparent wood is lightweight and has low cost, so it is a potential material for light-transmitting buildings and transparent solar cell windows. In the same year, Zhu et al.[3] fabricated the transparent wood with a high optical transmittance (up to 90%) and a high haze (up to 80%) by removing lignin contents from basswood and immersing wood in PVP solution under a range of conditions. Then they attached the transparent wood to the GaAs cell firmly. This attachment contributed to the effective light scattering and increased light absorption in the solar cell, so the total energy conversion efficiency increased by 18%. In the latest research, in order to make transparent wood to be better used in buildings and optical devices, researchers continue to give transparent wood multifunctionalities: functional nanoparticles are added to the polymer, which is used to fill the nanoscale wood template. For example, Gan et al. added γ-Fe_2O_3@YVO_4:Eu^{3+} nanoparticles to a polymer to form a new type of luminescent transparent wood composite. This material has great potential in applications including green LED lighting equipment, luminescent magnetic switches, and anticounterfeiting facilities.[4] In the same year, Yu et al. dispersed Cs_xWO_3 nanoparticles in a prepolymerized resin and filled them in the nanopores of delignified wood to obtain transparent wood. The wood-based composite exhibits excellent near-infrared shielding capability and high light transmission, which is also a potential material for smart window applications.[5]

In recent years, the process of preparing transparent wood has become more mature, and the performance test has been comprehensive and meticulous. Through the study of the domestic and foreign literature, it is found that most of the current research directions are based on the concepts of reducing energy consumption, paying attention to energy

Received: August 11, 2019
Accepted: November 12, 2019
Published: January 22, 2020

© 2020 American Chemical Society

DOI: 10.1021/acsomega.9b02498
ACS Omega 2020, 5, 1782−1788

conservation, and environmental protection.[6] Then, based on the inspiration of the frontier topic of transparent wood, if we change the angle, for the home industry, in the face of the continuous expansion of the field of household materials and the demand for new materials in the home decoration design, wood with translucency is also an excellent functional decorative material.

The transparent wood mentioned in the above literature is delignified; however, Li et al.[7] stated that lignin accounts for about 30% of wood and cross-links with different polysaccharides in wood to give structural support. The removal of lignin weakens the wood structure to a certain extent, limits the fabrication of large structures, and also limits the choice of tree species for the preparation of transparent wood.[8] For example, pine, poplar, and other low-density tree species are easily broken after lignin removal.[9] At this time, Li et al.[10] proved that delignification is not the necessary step to fabricate transparent wood products. Therefore, inspired by this conclusion, in this study, all sample preparation retained lignin. Retaining lignin not only makes the production process faster and more energy-saving but also enriches the color and texture of home decoration materials. At the same time, in order to enhance the practicality of the research and effectively expand the types of home decoration materials, six common tree species with different densities were selected in the experiment, and transparent wood with different colors and patterns was prepared for all tree species (not necessarily completely transparent). Besides, a series of performance studies and comparative analysis were carried out on them.

2. EXPERIMENTAL SECTION

2.1. Materials. The samples used were six kinds of wood veneers obtained from Yihua Lifestyle Technology Co., Ltd., China. These six species are *Betula alnoides* (*Betula*, A), Chinese fir (*Cunninghamia konishii* Hayata, B), basswood (*Tilia*, C), New Zealand pine (*Pinus radiata D.Don*, D), oguman (*Aucoumea klaineana*, E), and black walnut (*Juglans nigra*, F). The samples were cut to 20 mm × 20 mm with a thickness range of 0.15−0.51 mm and are shown in Figure 1. In order to facilitate the interpretation of the article, the above six tree species are denoted as A, B, C, D, E, and F from left to right. For these tree species, the original wood before the experiment was collectively referred to as OW. The air-dry densities and relative water contents of the six wood species are shown in Table 1. Chemical reagents (analytical grade) used are the following: ethanol absolute was produced by Guangdong Guanghua Sci-Tech Co., Ltd. Azobisisobutyronitrile (AIBN) was supplied by Tianjin Benchmark Chemical Reagent Co., Ltd. Methyl methacrylate (MMA) and sodium hydroxide (NaOH) were all supplied by Xilong Scientific Co., Ltd.

Figure 1. Samples A−F of different species (color ranges from deep to light).

Table 1. Physical Properties of Different Tree Species

wood species	air-dry density relative (g/cm^3)	water content (%)	thickness (mm)
B. alnoides (A)	0.65	9.98	0.51
Chinese fir (B)	0.39	11.37	0.40
basswood (C)	0.44	8.59	0.43
New Zealand pine (D)	0.31	10.03	0.50
oguman (E)	0.30	9.31	0.15
black walnut (F)	0.49	9.79	0.44

2.2. Fabrication of Transparent Wood. First of all, six different kinds of wood veneer samples were heated in an oven at 103 °C for 24 h and then stored in a drying dish. In further experiments, in order to avoid the mutual influence between different tree species and errors in the results of the experiment, the sample impregnation test for each wood species was done independently (the fabrication of transparent wood for six wood species is consistent).

As shown in Figure 2, before impregnation, the dried wood was placed in the ethanol absolute solution to displace the moisture inside, which greatly enhanced the permeability of the wood.[11,12] NaOH solution was used to remove the polymerization inhibitor inside the pure MMA monomer. Then the MMA monomer was prepolymerized in a water bath at 75 °C for 15 min with 0.35 wt % AIBN as the initiator. After 15 min, the prepolymerized MMA solution was cooled to room temperature in an ice water bath to terminate the reaction. Next, the wood in the ethanol absolute solution was taken out and immersed in the prepolymerized resin solution prepared above for half an hour under vacuum, and then the infiltrated wood was stood for a period of time to ensure that it was completely wetted. At last, the infiltrated wood was clamped between two glass slides and packaged in aluminum foil before further polymerization. The further polymerization reaction was finished by putting the infiltrated wood sample in an oven at 70 °C for 5 h.[2] For the above six tree species, the transparent wood after the experiment was collectively referred

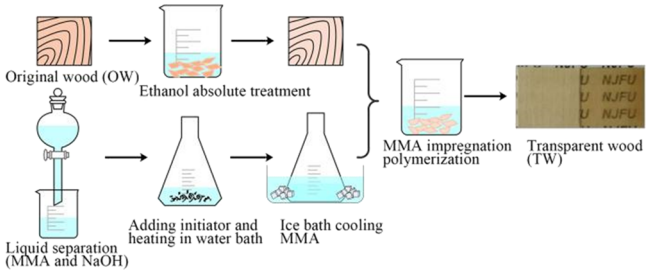

Figure 2. Main flowchart of transparent wood fabrication.

DOI: 10.1021/acsomega.9b02498
ACS Omega 2020, 5, 1782−1788

to as TW. If it refers to a wood species specifically, taking the *B. alnoides* as an example, it is called OW-A before the experiment and TW-A after the experiment, and so, tree species Chinese fir (B), basswood (C), New Zealand pine (D), oguman (E), and black walnut (F) are called OW-B, OW-C, OW-D, OW-E, and OW-F before the impregnation and TW-B, TW-C, TW-D, TW-E, and TW-F after the impregnation.

2.3. Color Difference Test. A color reader (CR-10) was used to test the color difference between the original wood (OW) and the transparent wood (TW). For each tree species, the average values of five samples were tested before and after the experiment. Moreover, the sample color selection of each tree species should be as consistent as possible, reducing experimental errors. Here, the material was selected from the same part of the tree species. The color reader uses the *L*, *a*, and *b* three parameters for the sample readings. The *L* value reflects the brightness (0 means black, 100 means white); the larger the *L* value is, the higher the brightness is. The *a* value reflects the red-green degree (positive value is red, negative value is green), and the *b* value reflects the orange-blue degree (positive value is orange, negative value is blue). The color is deeper with the greater absolute value of *a* or *b*.[13]

2.4. Light Transmittance Test. Light transmittance of samples was measured by an ultraviolet−visible spectrophotometer (Shanghai Yoke UV1900PC) under light of 350−800 nm wavelength.

2.5. Scanning Electron Microscopy. An FEI Quanta 200 scanning electron microscope (SEM) was used to observe the surface topography of OW and TW samples. In the experiment, the samples were cut longitudinally along the trunk, which was a chord section. In the microscopic structure, the inner fiber was parallel to the plane direction of the wood. In order to observe the tightness of the interface between the polymer and the wood fiber more clearly, the samples were cut flat with a glass knife along the thickness direction and adhered to the copper sheet. After spraying gold, the samples were observed and measured by electron microscopy.

2.6. Fourier Infrared Test. Fourier transform infrared spectroscopy (FTIR) was used to obtain the infrared absorption spectra, and then the characteristic absorption peaks of OW and TW were compared to analyze the characteristics and causes of group and color changes before and after the OW and TW.

2.7. Mechanical Performance Test. The tensile properties of the wood samples before and after impregnation were measured. At least three repeats were tested for each wood species. The tensile properties of OW and TW were measured by using a computer-controlled electronic universal testing machine (SANS-CMT6104). The machine stretched in the direction of the wood grain, and the speed was set to 2 mm/min.

3. RESULTS AND DISCUSSION

3.1. Color Difference Classification and Analysis. For the three variable values *L*, *a*, and *b* involved in the color difference test, the samples OW of different wood species are first divided into two categories based on *L*. The species with *L* values of 45−55 are group X: black walnut (F), Chinese fir (B), and *B. alnoides* (A); the species with *L* values of 65−85 are group Y: oguman (E), New Zealand pine (D), and basswood (C). It can be intuitively found that the wood color of group X with lower *L* values is darker than that of group Y. As shown in Figure 3, before and after the impregnation, the *a* and *b* values of the TW samples showed irregular changes, among which *L* values changed regularly. The *L* values of all samples decreased, and the brightness decreased. The numerical analysis shows that, after experimental modification,

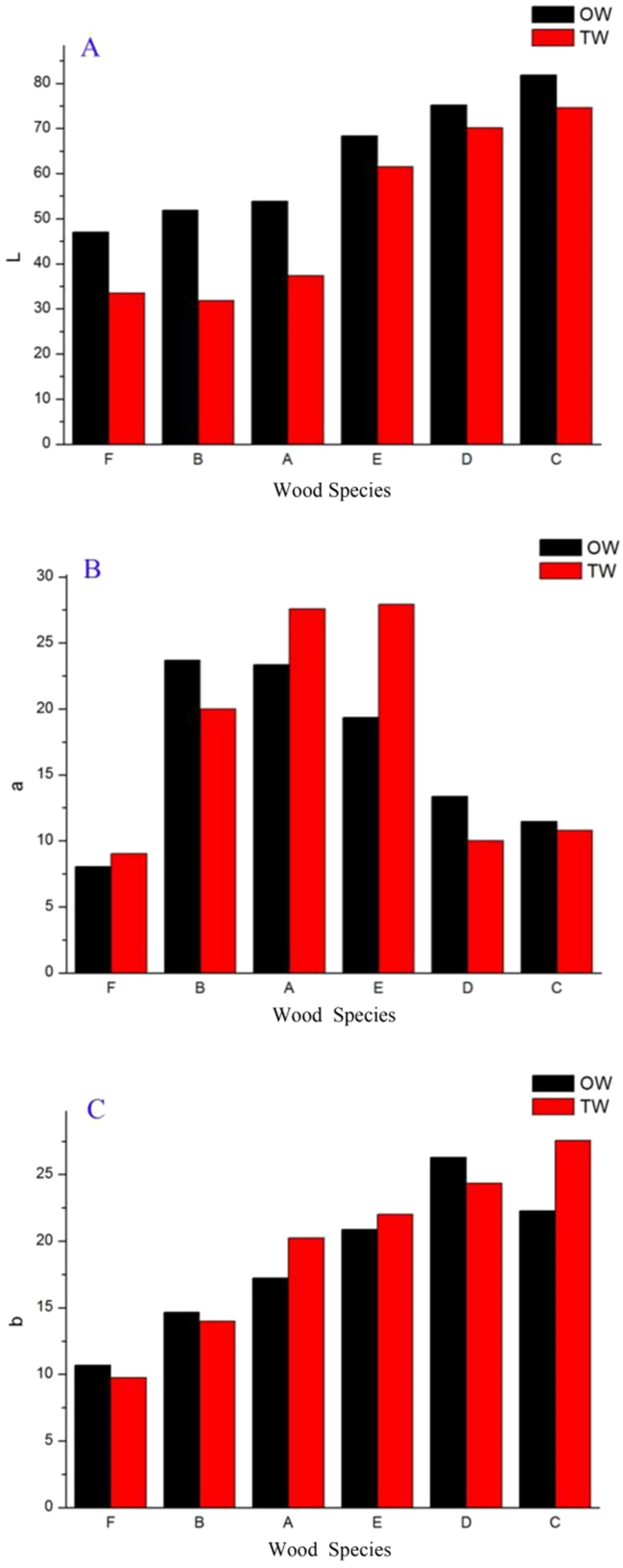

Figure 3. Surface colors of the OW and TW ((A) *L* value; (B) *a* value; (C) *b* value).

DOI: 10.1021/acsomega.9b02498
ACS Omega 2020, 5, 1782−1788

the values of the three parameters have changed, and there is no constant quantity. It can be seen that only light and shade will change in the end, and the hue will not change dramatically.[14] The reason for the decrease in brightness is that, in the colored phase, the brightness of yellow is high, the brightness of red and blue is low, and the main chromogenic substance in wood is lignin. The higher the content of lignin, the more inclined to yellow, the higher the brightness.[15] Because the filling and aggregating of resin reduced the proportion of original lignin in the sample, the brightness of the sample decreased after the impregnation test. The above reflects the variation law and trend of color differences before and after impregnation of different tree species.

3.2. Light Transmittance Analysis. As can be seen from Figure 4, the light transmittance of TW significantly improved

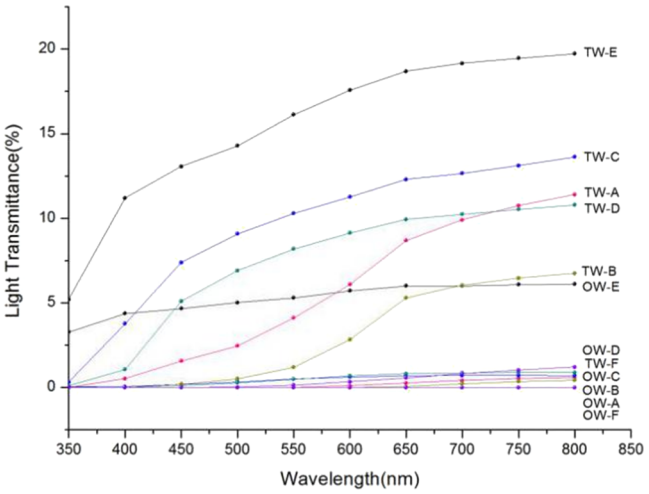

Figure 4. Light transmittances of OW and TW.

at the wavelength range of 400−800 nm by experimental modification; especially for the tree species with low density and light color, such as C, D, and E, the maximum increase of transmittance can reach 13−14%. For F, the light transmittance increased only slightly at the wavelength range of 500−800 nm because of the high density of the tree species and the deep color of the wood.[16] It can be seen that the light transmittance of TW prepared by light-colored tree species increased more significantly. Since the light-transmissive wood (TW) prepared in this paper is intended to retain the color and texture of wood to a certain extent, lignin or other chromophoric substances are not removed, and thus, the transmittance values of the modified samples are lower than those of some completely transparent woods. As shown in Figure 5, although these samples including TW-A, TW-B, TW-C, TW-D, TW-E, and TW-F do not show high light transmittance or high haze in daylight (samples were placed on paper printed with "NJFU"), these woods exhibit unique advantages and aesthetics under specific light conditions: they can transmit light and have the natural color and texture of wood, which is innovative and shows the potential to be an excellent functional decorative material.

3.3. SEM Analysis. Figure 6a−d shows the SEM images of OWC and TWC at different magnifications. SEM showed that OW had honeycomb-like holes, and there were obvious gaps between cell walls.[17,18] Figure 6c,d shows that the holes of wood such as conduits and pits were filled with resin and the

Figure 5. Contrast photos of OW-A, TW-A, OW-B, TW-B, OW-C, TW-C, OW-D, TW-D, OW-E, TW-E, OW-F, and TW-F samples in daylight and specific light conditions.

surface was smooth and flat. Because of the filling and polymerization of resin, the interfacial gap between PMMA and wood fibers was reduced, and the cell walls fit snugly to each other. Meanwhile, the porous structure of wood was almost eliminated. In addition, other tree species were consistent with this phenomenon. These results demonstrate that PMMA and wood template are successfully aggregated and interact with each other. Because the wood cell wall is similar to the refractive index of the impregnated resin (≈1.5), according to the theorem the closer the refractive index of the two media is, the smaller the reflectance is, the larger the transmittance is, so the light-transmissive composite material can be obtained with the resin curing in the wood template.[19]

3.4. Fourier Infrared Analysis. Figure 7a shows the infrared spectrum of OW. The characteristic absorption peaks presented include 3330 (O−H stretching vibration), 2930 (C−H stretching vibration), 1740 (C=O stretching vibration), 1735 (acetyl site of hemicellulose), 1700 (fatty acid in extract), 1505 (aromatic nucleus skeleton of lignin), and 1034 cm^{-1} (ether bond of cellulose). The above is consistent with the research in the existing literature.[20,21] For A−F, although the tree species are different, as wood, the main components are similar, so the main stretching vibration points of the spectrum are basically the same. The absorption peaks that exist have differences in the degrees of height due to different contents of components at the same point for A−F, but it does not affect the judgment of components.

The infrared spectrum of the TW after resin impregnation polymerization not only retains some characteristic absorption peaks of the OW but also has the characteristic absorption peaks of PMMA (2992 and 2950 cm^{-1} for C−H, 1740 cm^{-1} for C=O, and 1191 and 1145 cm^{-1} for C−O),[22] as shown in Figure 7b. It shows that PMMA and wood have an excellent polymerization effect, and although A−F are six different tree species, the changes of characteristic peaks tend to be consistent under the same experimental conditions, indicating that this experiment can be applied to many tree species.

3.5. Mechanical Performance Analysis. The tensile strength was calculated by the following equations:

$$\sigma = \frac{F}{S} \quad (1)$$

$$S = b \times h \quad (2)$$

DOI: 10.1021/acsomega.9b02498
ACS Omega 2020, 5, 1782−1788

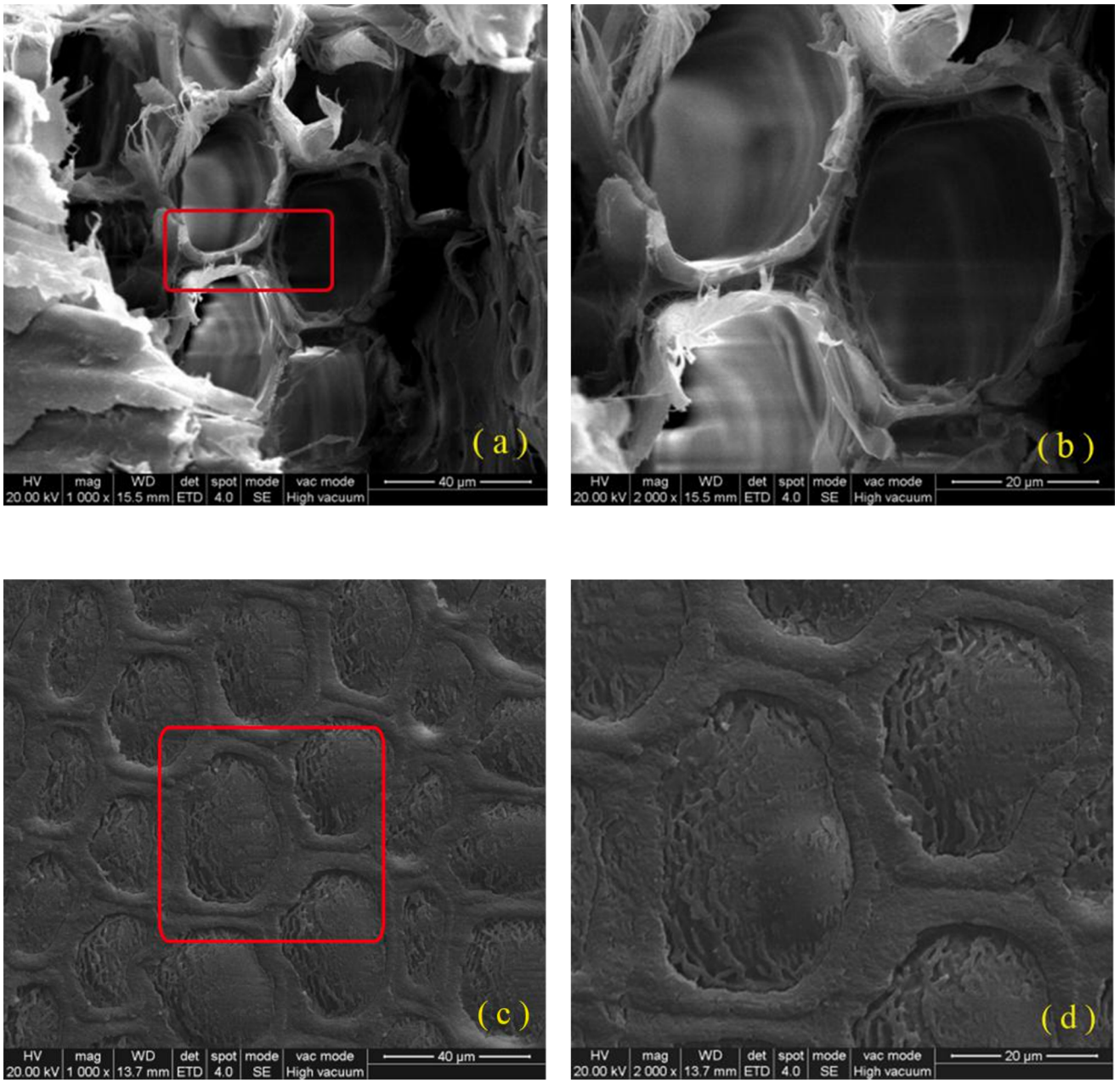

Figure 6. SEM images of OWC (a,b) and TWC (c,d).

where σ (MPa) is the tensile strength, which represents the maximum load carrying capacity of the sample under static tensile conditions, F is the maximum force that the sample is subjected to when it is broken, S is the original cross-sectional area in the tensile direction of the sample, b is the initial width of the tensile section of the sample, and h is the initial thickness of the tensile section.[16,23]

Figure 8 shows a mechanical tensile load−displacement diagram: during the stretching process, the sample underwent an elastic deformation stage, a yield stage, and a plastic deformation stage and broke finally. Because of the load dropping sharply at the moment of the fracture and the displacement stopping at the same time (the displacement that stopped at the moment of force disappearance was the setting of the testing machine before the experiment), the F value of the sample should be at the highest point of the curve. Each sample was tested three to five times, and the mean value of F was calculated. Then a series of σ values were obtained according to the formula.[24]

The σ values of OW and TW for different tree species are plotted as images for comparative analysis. As can be seen in Figure 9, the tensile strengths of all tree species increased significantly, but the tree species were different and the increase was different. The most notable is that of A; TW has a 40% improvement in mechanical performance compared to OW; the smallest increase is B, and the mechanical performance of TW is 9% higher than that of OW. Therefore, according to the data analysis, compared with OW, TW generally has higher strength and ductility after PMMA penetration. It also shows macroscopically that resin and wood have a good synergistic effect, thus improving the overall mechanical properties.

DOI: 10.1021/acsomega.9b02498
ACS Omega 2020, 5, 1782−1788

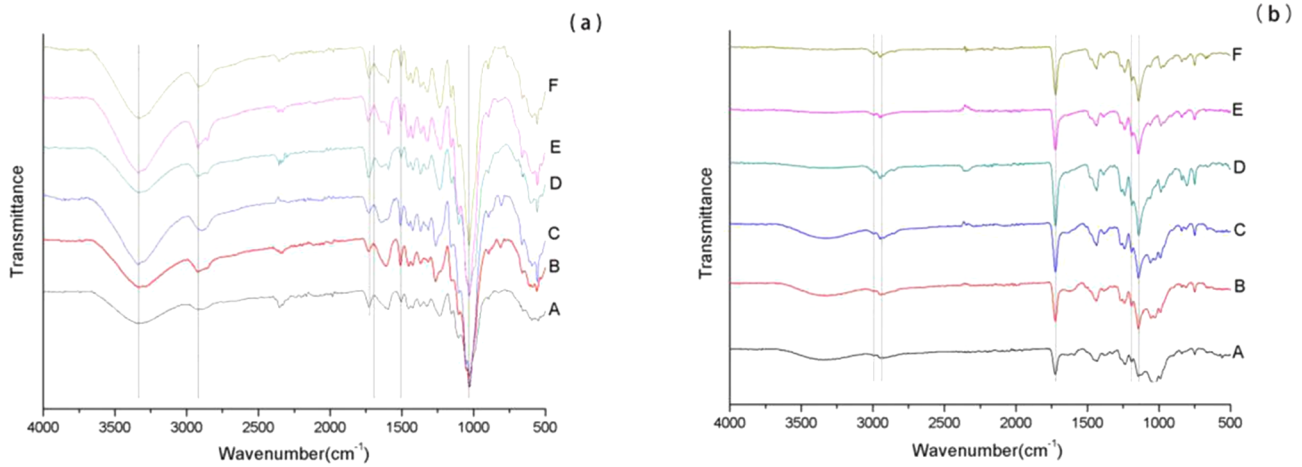

Figure 7. FTIR spectra of OW (a) and TW (b).

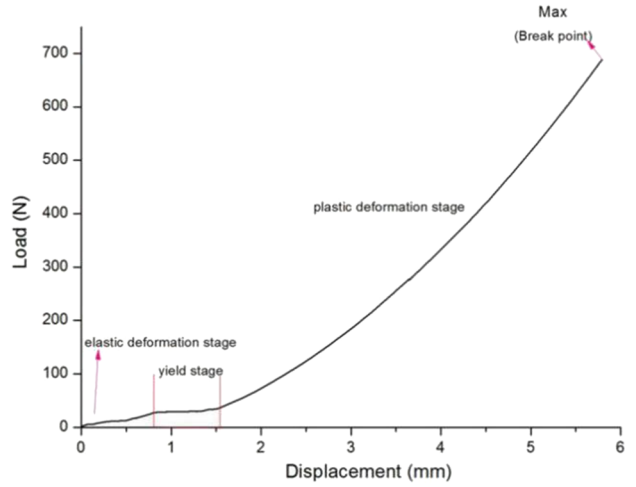

Figure 8. Mechanical tensile load−displacement diagram.

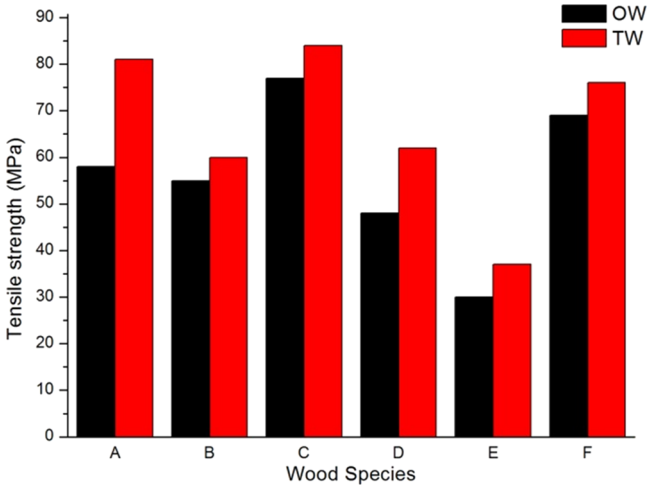

Figure 9. Tensile strengths of OW and TW.

4. CONCLUSIONS

Both microscopic analysis and mechanical testing revealed a good synergistic effect between wood and PMMA. The light transmittance and tensile strength of some tree species increased by 14 and 40%, respectively. Although the specific values are different, the multiple species show the same trend, indicating that this experiment is widely applicable to various kinds of wood. The lignin is retained during the experiment so that the transparent wood has the color and texture of natural wood, while producing is faster and more energy-efficient. In the past literature, based on the perspective of energy saving and consumption reduction, transparent wood can be used as optical and electrical devices; here, for the home industry, which has been constantly expanding in the field of materials, it is found that transparent wood is also a highly potential functional decorative material. Finally, the difference in color and light transmittance of transparent wood prepared by dark and light tree species may be caused by different factors such as lignin content, pigment group, and extract type. The study of these blocks will be discussed in detail in future experiments.

AUTHOR INFORMATION

Corresponding Authors

*E-mail: wuyan@njfu.edu.cn (Y.W.).
*E-mail: yangfeng@bift.edu.cn (F.Y.).

ORCID

Jichun Zhou: 0000-0002-3116-9349
Feng Yang: 0000-0002-1045-0449

Funding

The authors gratefully acknowledge the financial support from the projects funded by Yihua Lifestyle Technology Co., Ltd. (YH-NL-201507 and YH-JS-JSKF-201904003) and the Special Scientific Research Fund of Construction of High-level Teachers Project of the Beijing Institute of Fashion Technology (BIFTQG201805).

Notes

The authors declare no competing financial interest.

ACKNOWLEDGMENTS

The authors gratefully acknowledge the financial support from P. R. China and would like to thank Shang Huang for helping us prepare the samples.

REFERENCES

(1) Zhu, M.; Song, J.; Li, T.; Gong, A.; Wang, Y.; Dai, J.; Yao, Y.; Luo, W.; Henderson, D.; Hu, L. Highly Anisotropic, Highly Transparent Wood Composites. *J. Adv. Mater.* **2016**, *28*, 5181−5187.
(2) Li, Y.; Fu, Q.; Yu, S.; Yan, M.; Berglund, L. Optically Transparent Wood from a Nanoporous Cellulosic Template:

DOI: 10.1021/acsomega.9b02498
ACS Omega 2020, 5, 1782−1788

Combining Functional and Structural Performance. *Biomacromolecules* **2016**, *17*, 1358.
(3) Zhu, M.; Li, T.; Davis, C. S.; Yao, Y.; Dai, J.; Wang, Y.; AIQatari, F.; Gilman, J. W.; Hu, L. Transparent and Haze Wood Composites for Highly Efficient Broadband Light Management in Solar Cells. J. *Nano Energy* **2016**, *26*, 332−339.
(4) Gan, W.; Xiao, S.; Gao, L.; Gao, R.; Li, J.; Zhan, X. Luminescent and Transparent Wood Composites Fabricated by Poly(methyl methacrylate) and γ-Fe_2O_3@YVO_4:Eu^{3+} Nanoparticle Impregnation. *ACS Sustainable Chem. Eng.* **2017**, *5*, 3855−3862.
(5) Yu, Z.; Yao, Y.; Yao, J.; Zhang, L.; Chen, Z.; Gao, Y.; Luo, H. Transparent Wood Containing Cs_xWO_3 Nanoparticles for Heat-shielding Window Applications. J. *J. Mater. Chem. A* **2017**, *5*, 6019−6024.
(6) Montanari, C.; Li, Y.; Chen, H.; Yan, M.; Berglund, L. A. Transparent Wood for Thermal Energy Storage and Reversible Optical Transmittance. *ACS Appl. Mater. Interfaces* **2019**, *11*, 20465−20472.
(7) Li, Y.; Fu, Q.; Rojas, R.; Yan, M.; Lawoko, M.; Berqlund, L. Lignin-retaining Transparent Wood. *ChemSusChem* **2017**, *10*, 3445−3451.
(8) Yang, T.; Cao, J.; Ma, E. How Does Delignification Influence the Furfurylation of Wood. *Ind. Crops Prod.* **2019**, *135*, 91−98.
(9) Wu, Y.; Tang, C.; Wu, J.; Huang, Q. T. Research Progress of Transparent Wood: a Review. *J. Forest. Eng.* **2018**, *3*, 12−18.
(10) Li, Y.; Fu, Q.; Rojas, R.; Yan, M.; Lawoko, M.; Berqlund, L. A New Perspective on Transparent Wood: Lignin-retaining Transparent Wood. *ChemSusChem* **2017**, *10*, 3445−3451.
(11) Jiankun, Q.; Tian, B.; Yali, S.; Xin, Z.; Shuai, L.; Yingcheng, H. Fabrication and Characterization of Multilayer Transparent Wood of Different Species. *J. Beijing Forest. Univ.* **2018**, *40*, 113−120.
(12) Murr, A. The Relevance of Water Vapour Transport for Water Vapour Sorption Experiments on Small Wooden Samples. *Transp. Porous Media* **2019**, *128*, 385−404.
(13) Lin, S.; Zhang, Q.; Yu, J.; Duan, H. Analysis of Relationship between Chromatic Aberration Value and Pigment Content of Peel in Different Peach Varieties. *Acta Agriculturae Jiangxi* **2018**, *30*, 35.
(14) Mottonen, V.; Karki, T. Color Changes of Birch Wood During High-Temperature Drying. *Drying Technol.* **2008**, *26*, 1125−1128.
(15) Tang, C. Y.; Wu, Y.; Wu, J. M.; Huang, Q. T.; Chen, H. Research on the Transparent Wood Composites-Process Optimization of Delignification. *Furniture* **2018**, *39*, 16−21.
(16) Wu, J.; Wu, Y.; Yang, F.; Tang, C.; Huang, Q.; Zhang, J. Impact of Delignification on Morphological, Optical and Mechanical Properties of Transparent Wood. *Composites, Part A* **2019**, *117*, 324−331.
(17) Ma, J.; Ji, Z.; Zhou, X.; Zhang, Z.; Xu, F. Transmission Electron Microscopy, Fluorescence Microscopy, and Confocal Raman Microscopic Analysis of Ultrastructural and Compositional Heterogeneity of Cornus Alba L. Wood Cell Wall. J. *Microsc. Microanal.* **2013**, *19*, 243−253.
(18) Gierlinger, N. Chemical Imaging of Poplar Wood Cell Walls by Confocal Raman Microscopy. *J. Plant Physiol.* **2006**, *140*, 1246−1254.
(19) Wang, Y.; Fu, S. Research Progress in Transparent Wood. *J. China Pulp & Paper* **2018**, *37*, 68−72.
(20) Gierlinger, N.; Goswami, L.; Schmidt, M.; Burgert, I.; Coutand, C.; Rogge, T.; Schwanninger, M. In Situ FT-IR Microscopic Study on Enzymatic Treatment of Poplar Wood Cross-sections. *Biomacromolecules* **2008**, *9*, 2194−2201.
(21) Rana, R.; Langenfeld-Heyser, R.; Finkeldey, R.; Polle, A. FTIR Spectroscopy, Chemical and Histochemical Characterisation of Wood and Lignin of Five Tropical Timber Wood Species of the Family of Dipterocarpaceae. *J. Wood Sci Technol* **2010**, *44*, 225−242.
(22) Kavale, M. S.; Mahadik, D. B.; Parale, V. G.; Wagh, P. B.; Gupta, S. C.; Rao, A. V.; Barshilia, H. C. Optically Transparent, Superhydrophobic Methyltrimethoxysilane Based Silica Coatings without Silylating Reagent. *J. Appl. Surf. Sci.* **2011**, *258*, 156−162.
(23) Yusof, N. M.; Tahir, P. M.; Lee, S. H.; Khan, M. A.; James, R. M. S. Mechanical and Physical Properties of Cross-Laminated Timber Made from Acacia Mangium Wood as Function of Adhesive Types. J. *J. Wood. Sci.* **2019**, *65*, 20.
(24) Mang, H. A. On Special Points on Load-displacement Paths in the Prebuckling Domain of Thin Shells. *J. Int. J. Numer. Meth. Eng.* **2010**, *31*, 207−228.

DOI: 10.1021/acsomega.9b02498
ACS Omega 2020, 5, 1782−1788